Structural Brain Changes in Pre-Clinical FTD *MAPT* Mutation Carriers

Clara Domínguez-Vivero[a,*], Liwen Wu[b], Seonjoo Lee[b], Masood Manoochehri[a], Sarah Cines[a,f],
Adam M. Brickman[a], Batool Rizvi[a], Anthony Chesebro[a], Yunglin Gazes[a], Emer Fallon[d],
Timothy Lynch[d], Judith L. Heidebrink[e], Henry Paulson[e], Jill S. Goldman[a], Edward Huey[a,c]
and Stephanie Cosentino[a]

[a]*Department of Neurology, Columbia University, Cognitive Neuroscience Division of the Taub Institute,
G.H. Sergievsky Center, New York, NY, USA*
[b]*Department of Biostatistics, Columbia University, Mailman School of Public Health, New York, NY, USA*
[c]*Department of Psychiatry & New York State Psychiatric Institute, Columbia University, New York, NY, USA*
[d]*Dublin Neurological Institute, Dublin, Ireland*
[e]*Department of Neurology, The University of Michigan, Ann Arbor, MI, USA*
[f]*Fairleigh Dickinson University, Teaneck, NJ, USA*

Abstract.

Background: Frontotemporal dementia (FTD) is the second most common cause of early-onset neurodegenerative dementia. Several studies have focused on early imaging changes in FTD patients, but once subjects meet full criteria for the FTD diagnosis, structural changes are generally widespread.

Objective: This study aims to determine the earliest structural brain changes in asymptomatic *MAPT* MUTATION carriers.

Methods: This is a cross-sectional multicenter study comparing global and regional brain volume and white matter integrity in a group of *MAPT* mutation preclinical carriers and controls. Participants belong to multiple generations of six families with five *MAPT* mutations. All participants underwent a medical examination, neuropsychological tests, genetic analysis, and a magnetic resonance scan (3T, scout, T1-weighted image followed by EPI (BOLD), MPRAGE, DTI, FLAIR, and ASL sequences).

Results: Volumes of five cortical and subcortical areas were strongly correlated with mutation status: temporal lobe (left amygdala, left temporal pole), cingulate cortex (left rostral anterior cingulate gyrus, right posterior cingulate), and the lingual gyrus in the occipital lobe. We did not find significant differences in whole brain volume, white matter hyperintensities volume, and white matter integrity using DTI analysis.

Conclusion: Temporal lobe, cingulate cortex and the lingual gyrus seem to be early targets of the disease and may serve as biomarkers for FTD prior to overt symptom onset.

Keywords: Atrophy, brain atrophy, early detection, frontotemporal lobar degeneration, *MAPT* mutation

INTRODUCTION

Frontotemporal dementia (FTD) is the second most common cause of early-onset neurodegener-

ative dementia [1]. Up to 40% of FTD cases are associated with an autosomal dominant pattern of inheritance. Mutations in over eight genes have been identified in FTD, including progranulin (*GRN*), chromosome 9 open reading frame (*C9orf72*), and microtubule-associated protein tau (*MAPT*) genes [2, 3]. Neuroimaging has been explored as a potential biomarker to identify patients in initial phases of

*Correspondence to: Clara Dominguez, MD, 630 West 168th Street, P&S Box 16, New York, NY 10032, USA. Tel.: +1 212 305 1134; E-mail: claradominguezvivero@gmail.com.

neurodegenerative diseases and to measure biological change over time [4]. Several studies have focused on early imaging changes in FTD patients [5–10], but once subjects meet full criteria for FTD diagnosis, structural changes are generally widespread [11]. Studying mutation carriers who are asymptomatic or transitioning from asymptomatic to symptomatic (what we will refer to as "preclinical") [12] may allow for characterization of the earliest neuroimaging changes in disease [13–17].

Studies specifically addressing preclinical neuroimaging features in *MAPT* mutation carriers are scarce. Some studies [18, 19] have demonstrated early insular atrophy, and others early medial temporal degeneration [20, 21]. Also, some studies have reported early white matter changes in preclinical FTD patients [22–25], but those performed specifically in *MAPT* mutation carriers have not [26]. Our institution has access to a relatively large, broadly phenotyped group of *MAPT* mutation carriers and familial matched controls that brings the opportunity to study early imaging changes in a well characterized population to address the inconsistencies found in previous studies. With that purpose, we compare cortical and subcortical gray matter volumes as well as white matter hyperintensities and tract-integrity between *MAPT* mutation carriers and demographically-matched familial controls.

MATERIALS AND METHODS

Participants

Participants were recruited from an active, longitudinal research protocol (R01NS076837) that includes multiple generations of six families with *MAPT* mutations: V337M (c.2014G>A), P301L (c.1907C>T), Exon 10 + 14 *C* > T, Exon 10 + 15 *C* > T, and Exon 10 + 16 *C* > T. Members of these families live throughout areas of the United States and Europe. Those who consented to participate in the study were followed at Columbia University Medical Center, the University of Michigan, and the Dublin Neurological Institute.

Sixty subjects were enrolled and 56 completed the baseline visit, during which genetic, biological, neuroimaging, and clinical data were collected. Four subjects did not complete the study due to rejection to undergo all the exams. No imaging studies were rejected for the analysis due to quality issues. Sample characteristics are displayed in Table 1.

Clinical assessments

Most participants, and investigators whenever possible, were blind to carrier status. A full history and physical and neurological examination was performed by one of the study physicians at the enrolling clinical site. The Clinical Dementia Rating (CDR) Scale, including the language and behavior components (CDR® Plus NACC FTLD), as well as cognitive, behavioral, and psychiatric measures was completed as part of this evaluation (Table 1). Informants provided input for the clinical assessment and participated in the completion of behavioral interviews administered by the study coordinator. Participant cognitive status was characterized using tests from the National Alzheimer's Coordinating Center (NACC) UDS 2.0 Neuropsychological Battery and NACC UDS 2.0 FTLD Module. This evaluation included assessment of memory function (Mini-Mental State Examination, Selective Reminding Test immediate and delayed recall, Selective Reminding Test discriminability index), verbal function (categorical fluency, Boston Naming Test, Controlled Oral Word Association (COWA)), visual cognition (Benson figure), executive function (Trail A, Trail B, COWA, 20 Q's, Design Fluency, Graphic Pattern Generation), social abilities (Social Norms Questionnaire 22, Empathic Concern Score, Perspective Taking Score, Revised Self-Monitoring Scale), other frontal lobe functional tests (Remote Associates Test) as well as depression and anxiety (Neuropsychiatric Inventory).

Genetic analysis

Blood was collected through standard phlebotomy procedures at the Columbia University Medical Center (Irving Center for Clinical and Translational Research), University of Michigan, and the Dublin Neurological Institute. Fifteen cc of blood were collected, including citrate tubes for DNA isolation and heparin tubes for plasma isolation. DNA was prepared from whole blood using standard protocols in the Columbia Human Genetics Resources Core. Polymerase chain reaction (PCR) and amplification were performed in all samples. The PCR and sequencing primers used for amplification and sequencing were designed using the software Primer 3 (http://frodo.wi.mit.edu/primer3/). Cycle sequencing in forward and reverse directions was performed on purified PCR products and run on an ABI 3730 genetic analyzer (Applied Biosystems,

Table 1
Demographic information about age, gender, and education. Results of neuropsychological tests adjusted (by age, gender, and education). By Fisher exact test/2-sided Wilcoxon test, there is not significant difference of age, gender, and education between carriers and non-carriers

Clinical features	Non-carrier ($n = 44$)		Carrier ($n = 12$)		Carrier (CDR 0) ($n = 6$)		Carrier (CDR 0.5) ($n = 6$)	
Gender	Count	%	Count	%	Count	%	Count	%
Female	24	54.55	8	66.67	4	66.67	4	66.67
Male	20	45.45	4	33.33	2	33.33	2	33.33
	Mean	SD	Mean	SD	Mean	SD	Mean	SD
Age	44.64	13.40	48.83	13.37	39.00	11.52	58.67	5.32
Education	15.18	2.33	15.25	2.14	15.33	2.07	15.17	2.40
Neuropsychiatric tests	Mean	SD	Mean	SD	Mean	SD	Mean	SD
SNQ22	–0.29	0.94	–1.18	1.3	–1.12	1.77	–1.24	0.74
EC	–0.02	1.1	–0.45	1.12	0.17	1.3	–1.07	0.39
PT	0.08	1.09	–1.06	1.27	–0.4	1.42	–1.72	0.7
RSMS (Z-score)	–1.6	1.2	–2.67	1.94	–1.49	1.93	–3.86	1.11
SRT[1]	46.06	10.44	32.47	19.87	50.42	4.34	14.52	8.73
SRT[2]	48.33	8.81	37.62	18.22	53.26	6.16	21.98	10.26
MMSE	0.59	0.73	–0.25	1.45	0.25	1.13	–0.75	1.66
Cat. F (Animals)	–0.46	0.79	–1.32	1.27	–0.35	0.54	–2.28	1.01
Trail-A (Z-score)	–0.35	0.61	–1.09	1.41	–0.48	0.44	–1.69	1.82
Trail-B (Z-score)	–0.4	0.74	–0.89	1.01	–0.56	0.3	–1.23	1.37
BNT (Z-score)	–0.53	0.67	–2.81	2.67	–0.73	0.71	–4.88	2.2
Benson Figure Copy (Z-score)	0.73	1.03	0.31	1.2	0.59	1.05	0.03	1.37
CFL	47.2	9.32	42.25	12.06	47	9.36	37.5	13.35
SRT	0.97	0.04	0.87	0.19	0.99	0.03	0.75	0.21
20 Q's	11.69	2.48	10.17	3.33	12	1.79	8.33	3.61
RAT	15.98	0.15	15.17	1.34	15.83	0.41	14.5	1.64
DF	17.41	1.88	13.82	7.61	18.67	1.51	8	8.03
GPG[1]	6.83	4.07	3.7	4.6	3.7	4.6	3.7	5.14
GPG[2]	309.2	181.1	310.9	206.7	261.6	155.9	360.2	256.4

NPI*	Non-carriers ($n = 44$)	Carriers ($n = 12$)	Carriers CDR 0 ($n = 6$)	Carriers CDR 0.5 ($n = 6$)
Agitation	4.88%	45.45%	0.00%	83.33%
Anxiety	9.76%	40.00%	20.00%	60.00%
Apathy	2.44%	36.36%	0.00%	66.67%
Appetite	9.76%	27.27%	0.00%	50.00%
Delusions	2.44%	0.00%	0.00%	0.00%
Depression/dysphoria	9.76%	27.27%	20.00%	33.33%
Disinhibition	4.88%	45.45%	0.00%	83.33%
Elation	0.00%	27.27%	0.00%	50.00%
Hallucinations	0.00%	9.09%	0.00%	16.67%
Irritability	4.88%	36.36%	0.00%	66.67%
Motor disturbance	2.44%	18.18%	0.00%	33.33%
Nighttime behaviors	4.88%	18.18%	0.00%	33.33%

SNQ22, Social Norms Questionnaire (Z-score); EC, Interpersonal Reactivity Index Empathic Concern Score (Z-score); PT, Interpersonal Reactivity Index Perspective Taking Score (Z-score) RSMS, Revised Self-Monitoring Scale (Z-score); SRT[1], Immediate Recall T-score (total score); SRT[2], Delayed Recall T-score (Total score); MMSE, Mini-Mental State Examination Total score (Z-score); Cat.F Animals, Category Fluency for Animals (Z-score); Trail-A, Trail Making Test part A (Z-score); Trail-B, Trail Making Test part B (Z-score); BNT, Boston Naming Test (Z-score); Benson Figure (Z-score); CFL, Controlled Oral Word Association (COWA) Test using C, F, and L; SRT, Selective Reminding Test Discriminability index; 20 Q's, 20 questions from DKEFS Total Weighted Achievement - Scaled Score; RAT, Remote Associates Test Total Score; DF, Design Fluency total correct score; GPG[1], Graphic Pattern Generation Perseveration Distance; GPG[2], Graphic Pattern Generation Perseveration Time (in seconds), NPI, Neuropsychiatric Inventory. *3 non-carriers with CDR 0 (ES012, ES024, ES036) and 1 carrier with CDR 0 (ES038) do not have NPI-Q data.

Foster City, CA). Sequence chromatograms were viewed and genotypes determined using Sequencher (Genecodes). Samples were stored frozen at –80°C. Subjects did not receive DNA results as part of the current study. Patients were screened for mutations in other genes associated with FTD besides *MAPT*.

Imaging procedures

A number of imaging modalities were acquired during a 1 h magnetic resonance (MR) scan performed in NY and Dublin in a 3.0T Philips Achieva Quasar Dual Magnet using a 240 mm field of view.

A scout, T1-weighted image was first acquired to determine patient position, followed by echo planar imaging (blood oxygenation level dependent), magnetization-prepared rapid acquisition with gradient echo (MPRAGE), diffusion tensor imaging (DTI), fluid-attenuated inversion recovery (FLAIR), and arterial spin labeling sequences. The following parameters were used:

* T1-weighted: repetition time = 20 ms, echo time = 2.1 ms, field of view = 240 cm, and 256 ± 160 matrix with 1.3 mm slice thickness.
* FLAIR: repetition time = 11,000 ms, echo time = 144.0 ms, inversion time = 2800 ms, field of view = 25 cm, 2 NEX, and 256 ± 192 matrix with 3 mm slice thickness.
* DTI: repetition time = 11032 ms, echo time = 69 ms, acquisition time 6 mins, slice thickness 2 mm.

A neuroradiologist reviewed each subject's MRI scan for clinical abnormalities. Scanning procedures were standardized between all centers using methods previously described [27] conducted in person by a radiologist from CUMC. Structural imaging measures of global and regional brain volume were derived from each individual's T1-weighted MPRAGE image using Freesurfer software (http://surfer.nmr.mgh.harvard.edu/). For brain volume calculations, we used the procedures of Walhovd et al. [28] to automatically assign a neuroanatomical label to each voxel, with results comparable to manual labeling. From this labeling, volumetric regions of interest (ROIs) were defined. The calculated volume within each region was adjusted for variations in individual global brain volume with a measure of total intracranial volume (TIV). We decided to compare values of all the different areas, without defining ROIs *a priori*. This method allows an unbiased assessment of patterns of atrophy across the whole brain without limiting the number of potential measurements performed in the study [29]. In order to measure white matter hyperintensities, each participant's FLAIR image was skull stripped and after, voxel intensity values of the remaining image were analyzed using a Gaussian curve. Hyper-intense voxels were defined using a threshold of 2.1 SD above the mean intensity. They were labeled and measured in cubic centimeters multiplying the number of voxels for the voxel's dimensions.

DTI data was processed in FMRIB's Diffusion Toolbox (FDT), distributed as part of FMRIB's Software Library [30], by first preprocessing with eddy-current correction followed by fitting of the DTI model to the preprocessed data. To align all subjects into the same common space, tract-based spatial statistics [31] was run on the fractional anisotropy (FA) maps using the nonlinear registration tool FNIRT [32, 33] and then the mean FA image was created and thinned to create a mean FA skeleton, representing the centers of all tracts common to the group. Each subject's aligned FA data was then projected onto this skeleton and created a skeletonized map per subject. To extract 20 tracts of interest, Johns Hopkins University (JHU) white matter tractography atlas [34] was used as masks to obtain the mean FA for each tract for each participant.

Standard protocol approvals, registrations, and participant consents

Approval for this study was obtained from the appropriate IRB and ethics boards of Columbia and University of Michigan Medical Centers and the Dublin Neurological Institute. Written informed consent was obtained from all participants.

Statistical analysis

For statistical analysis, stats (v 3.3.0), glmnet (v 2.5.0) [35], and pROC (v 1.9.1) [36] packages implemented in R (v.3.3.1) were used. As a primary analysis, we hypothesized group differences in 16 bilateral subcortical, 68 bilateral cortical ROI volumes, and 5 white matter hyperintensity volumes (frontal, temporal, parietal, occipital, and basal ganglia). The volumetric measures were corrected for age and TIV. Group comparison between mutation carriers and non-carriers was conducted using Wilcoxon test followed by multiple comparison correction controlling for false discovery rate [37]. Wilcoxon test analysis followed by multiple comparison was also performed for each ROI for both CDR 0 and CDR 0.5 carriers, residualized for age and TIV. Regarding DTI results, group analysis was conducted on the mean FA for the 20 tracts to compare carriers versus non-carriers. Age was included as a covariate to remove the confound of age and correction for multiple comparisons was performed using the false discovery rate [37].

We also evaluated discriminability of the volumes using penalized logistic regression with elastic-net [38] and receiver operating characteristic (ROC) analysis, adjusted by clinical covariates. To select tuning parameters for elastic-net, leave-one-out cross

validation was used ($\alpha = 1$, $\lambda = 0.0469$). We did a 500 iteration bootstrapping to calculate the consistency of selecting each of the ROIs into the multivariate model.

RESULTS

We analyzed data from 56 participants belonging to five families carrying *MAPT* mutations. Twelve subjects were determined to be carriers of the following mutations: P301L (one subject), Exon 10 + 16 *C* > T (one subject), Exon 10 + 15 *C* > T (two subjects), V337M (c.2014G>A) (four subjects), and Exon 10 + 14 *C* > T (four subjects). Forty-four subjects were non-carriers. Demographic characteristics of the sample and performance in neuropsychological testing are displayed in Table 1. Subjects were considered preclinical if they did not fulfill FTD diagnostic criteria. We use the term "preclinical" rather than "presymptomatic" as this group includes those that scored 0 and 0.5 in CDR. CDR = 0 carriers had no cognitive or behavioral impairment, but all CDR = 0.5 carriers had one or more abnormal neuropsychological score, and most also had questionable or mild behavioral impairment as indicated on the Behavior, Comportment, and Personality rating of the CDR Supplemental scores (FTLD-CDR) [39]. However, as these abnormalities were considered as questionable by raters and they did not fulfill diagnostic criteria for FTD, patients with CDR score of 0.5 were included in the preclinical group. There were no significant differences in age, gender, and years of education between the groups.

For each ROI, Freesurfer-derived raw volumes were converted to percentage of TIV prior to the analyses. The resulting data were analyzed using two models, a Wilcoxon analysis and a multivariate elastic-net model. In Wilcoxon analysis, 32 of 89 measures show significant between-group differences after multiplicity adjustment (Table 2), including caudate, putamen, hippocampus, amygdala, *nucleus accumbens*, and several regions of the frontal and temporal lobes. Over 500 iteration bootstrapping, five measures were constantly selected (with over 80% selection rate), demonstrating a potential strong association with mutation status (Table 2, Fig. 1). These five ROIs are left amygdala (selection percentage 0.83), rostral anterior cingulate (selection percentage 0.91), posterior cingulate (selection percentage 0.81), temporal pole (selection percentage 0.92), and lingual volume (selection percentage 0.83). Among these five, the lingual area and posterior cingulate did not come out significant in Wilcoxon's test, likely because they are only strong predictors of mutation status when other ROIs are controlled. No significant difference was found in whole brain volume between mutation carriers and non-carriers. Results remained the same after recalculating bilateral selection percentage over 500 bootstrap iterations as when considering both hemispheres separately. Therefore, for those ROIs, the left and right sides were not competing. When considering the sum of ROIs on both sides, four measures were selected over 80% selection rate: white matter hyperintensities in the occipital lobe (selection percentage 0.862), temporal pole volume (selection percentage 0.97), lingual volume (selection percentage 0.876), and posterior cingulate volume (selection percentage 0.84).

We performed a subgroup analysis comparing CDR 0 and CDR 0.5 carriers (2-sided Wilcoxon Test after adjustment for multiple comparisons). We found significant differences in 18/89 measures after multiplicity adjustment with larger volumes in CDR 0 subgroup (shown in Table 3 with an ∗, values available in the Supplementary Table 1). Most of these ROIs are the same that were significantly different between carriers and non-carriers. Only left superior frontal gyrus (CDR0 = 1.26 versus CDR0.5 = 0.97, $p = 0.04$) and right precentral gyrus (CDR0 = 0.77 versus CDR0.5 = 0.63, $p = 0.049$) showed differences between CDR subgroups that were not present when comparing carriers and non-carriers. These results should be considered with caution, as the number of subjects for the subgroup analysis is very low.

We did not find significant differences between carriers and non-carriers in the volume of white matter hyperintensities. There was only a weak difference after adjusting results by age and TIV, which did not survive after adjustment for multiple comparisons and elastic-net analysis (Table 2). We found a significant difference for white matter hyperintensities in the basal ganglia between CDR 0 and CDR 0.5 preclinical carriers (CDR 0 = 2.69E–05 versus CDR 0.5 = 4.49E–06; $p = 0.03$) after adjustment for multiple comparisons.

DTI measures were available for 9 carriers and 40 controls due to technical issues during the neuroimaging exam. After comparing DTI results between groups, we found significant differences between carriers and non-carriers for the left cingulum at the cingulate gyrus (0.579 ± 0.055 versus 0.609 ± 0.034; $p = 0.041$), right cingulum at the cingulate gyrus
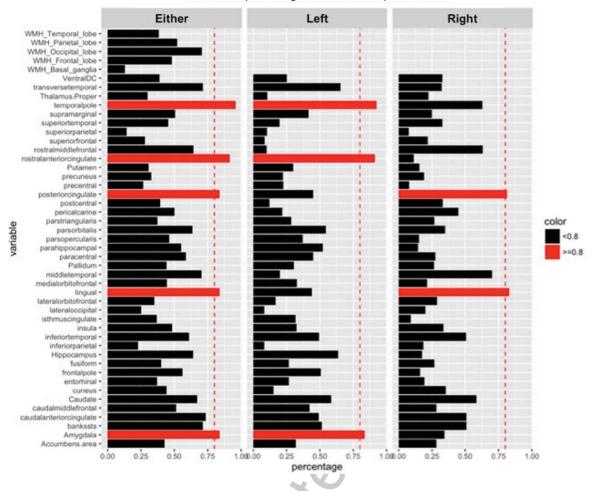
Table 2

Wilcoxon analysis and multivariate Elastic-net analysis. In Wilcoxon analysis 32/89 measures show significant between group differences after multiplicity adjustment. In Elastic-net model, 10/89 ROIs are selected into the model. Over 500 iteration bootstrapping, 5 measures are constantly selected (with over 80% selection rate) demonstrating a potential strong association with mutation status. The column 'Either' is a surrogate measure of the % selection for either left or right hemisphere of the specific ROI. When considering bilateral selection %, results remain the same as considering both hemispheres separately

Region	2-sided Wilcoxon test results				Percentage of selection		
White matter hyperintensities	Raw data		multiple adjustment: FDR (HL:<0.05)		over 500 Bootstrap iterations		
	Frontal_lobe 0.4129		0.4821		0.480		
Frontal_lobe	0.4129		0.4821		0.480		
Parietal_lobe	0.1909		0.2879		0.522		
Occipital_lobe	0.0634		0.2467		0.706		
Temporal_lobe	0.0515		0.0794		0.384		
WMH_Basal_ganglia*	0.1494		0.2770[1]		0.130		
Gray matter	Left	Right	Left	Right	Left	Right	Either
Thalamus.	0.1736	0.2151	0.1665	0.4349	0.106	0.222	0.298
Caudate	**0.0234**	**0.0396**	**0.0166**	**0.0223**	0.584	0.584	0.670
Putamen	**0.0246**	**0.0197**	**0.0243**	**0.0364**	0.298	0.156	0.306
Pallidum	0.4834	0.3081	0.7957	0.6757	0.304	0.264	0.442
Hippocampus	**0.0040**	**0.0186**	**0.0281**[1]	**0.0263**[1]	0.636	0.174	0.640
Amygdala	**0.0007**	**0.0137**	**0.0125**[1]	**0.0313**[1]	**0.834**	0.342	**0.838**
Accumbens area	**0.0074**	**0.0040**	**0.0405**	**0.0241**[1]	0.320	0.282	0.426
Ventral diencephalon	0.4236	0.4834	0.6564	0.7736	0.252	0.326	0.390
Banks of superior temporal sulcus	0.0918	**0.0208**	0.2233	**0.0271**	0.514	0.510	0.714
Caudal ant.Cingulate†	0.0999	0.4470	0.0815	0.4957	0.490	0.510	0.736
Caudal middle frontal	0.4470	**0.0233**	0.7605	0.0736	0.422	0.282	0.514
Cuneus	0.0770	0.1317	0.1362	0.2664	0.152	0.352	0.442
Entorhinal areal	**0.0057**	0.1228	**0.0192**	0.2326	0.266	0.192	0.372
Fusiform gyrus	0.0737	**0.0274**	0.0794	**0.0271**	0.268	0.266	0.402
Inf. parietal gyrus†	0.0558	0.1777	0.0949	0.2233	0.082	0.184	0.226
Inf. temporal gyrus	**0.0042**	**0.0030**	**0.0125**[1]	**0.0159**[1]	0.494	0.506	0.610
Isthmus cingulate	0.4122	0.5425	0.5165	0.9399	0.316	0.090	0.370
Lateral occipital gyrus	0.2987	0.4122	0.1360	0.4889	0.082	0.200	0.252
Lateral orbitofrontal	**0.0222**	**0.0131**	**0.0488**	**0.0166**[1]	0.168	0.286	0.348
Lingual gyrus	0.6012	0.9443	0.9399	0.5813	0.440	**0.828**	**0.838**
Medial orbitofrontal	**0.0305**	**0.0427**	**0.0488**	0.0736	0.326	0.212	0.444
Middle temporal	**0.0050**	**0.0030**	**0.0281**	**0.0125**[1]	0.200	0.700	0.702
Parahippocampal gyrus	0.0515	0.2677	**0.0488**	0.4089	0.522	0.146	0.552
Paracentral gyrus	0.1438	0.2805	0.2230	0.5165	0.448	0.274	0.586
Pars opercularis	0.1291	0.1438	0.1932	0.2099	0.372	0.152	0.460
Pars orbitalis	**0.0103**	0.0504	**0.0166**	0.1299	0.544	0.348	0.636
Pars triangularis	0.2120	0.0918	0.2716	0.2879	0.284	0.266	0.374
Pericalcarine gyrus	0.2463	0.3229	0.6757	0.5165	0.216	0.446	0.500
Postcentral gyrus	0.5605	0.3229	0.6634	0.5884	0.122	0.330	0.394
Post. cingulate gyrus¶	0.7007	0.8981	0.9764	0.9294	0.448	**0.814**	**0.838**
Precentral gyrus	0.3899	0.1317	0.4089	0.1362[1]	0.224	0.078	0.266
Precuneus	0.3683	0.2084	0.2517	0.2279	0.222	0.190	0.326
Rost. ant.cing. gyrus#	**0.0022**	0.1170	**0.0042**[1]	0.2056	**0.912**	0.112	**0.914**
Rostral mid.frontal gyrus**	0.0879	**0.0305**	0.0405	**0.0159**[1]	0.100	0.630	0.642
Superior frontal gyrus	0.0619	0.0613	0.0837[1]	0.0562	0.086	0.218	0.278
Superior parietal gyrus	0.1383	0.5605	0.0794	0.4154	0.102	0.076	0.142
Sup. temporal gyrus††	**0.0102**	**0.0068**	**0.0159**	**0.0141**[1]	0.196	0.328	0.454
Supramarginal gyrus	0.4352	**0.0131**	0.6757	**0.0488**	0.414	0.250	0.506
Frontal pole	0.7494	0.2048	0.6757	0.4089	0.506	0.160	0.560
Temporal pole	**0.0018**	**0.0195**	**0.0159**	**0.0313**[1]	0.924	0.628	**0.958**
Transverse temporal gyrus	0.0704	0.4236	0.1360	0.7736	0.654	0.322	0.712
Insula	**0.0260**	**0.0208**	**0.0159**[1]	**0.0488**[1]	0.324	0.334	0.484

The 5 ROIs are: left amygdala, left rostral anterior cingulate, left temporal pole, right lingual gyrus, and right posterior cingulate gyrus. Among these 5, right lingual gyrus and right posterior cingulate did not come out significant in Wilcoxon's test, probably because they are only a strong predictor of the mutation status when other ROIs are controlled. *White matter hyperintensities basal ganglia; †caudal anterior cingulate; †Inferior parietal gyrus; Inferior temporal gyrus; ¶Posterior cingulate gyrus; #Rostral anterior cingulate gyrus; **Rostral middle frontal gyrus; ††Superior temporal gyrus. [1]ROIs that showed significant differences between CDR 0 carriers and CDR 0.5 carriers.

Fig. 1. Multivariate analysis: Elastic net. Percentage of selection over 500 Bootstrap iterations. In Elastic-net model, 10/89 ROIs are selected into the model. Over 500 iteration bootstrapping, 5 measures are constantly selected (with over 80% selection rate), demonstrating a potential strong association with mutation status. This is a recalculation of selection percentage based on the bootstrap results. The column 'Either' is a surrogate measure of the % selection for either left or right hemisphere of the specific ROI. When considering bilateral selection %, the results remain the same as considering both hemispheres separately. It could be shown from the graph that for those ROIs, the bilateral ROIs seems not competing with each other.

(0.531 ± 0.053 versus 0.562 ± 0.038; *p* = 0.045), and left cingulum at the hippocampus (0.522 ± 0.074 versus 0.563 ± 0.047; *p* = 0.039). However, after adjusting these results for age, the differences were no longer significant.

DISCUSSION

In this study, we report early structural changes in pre-clinical *MAPT* mutation carriers measured using voxel-based morphometry and DTI analysis. Prior to overt symptom onset, *MAPT* mutation carriers in our sample showed volume differences in almost 30% of the 89 regions explored, including basal ganglia (cau-date, putamen), temporal lobe (in particular medial temporal lobe), and some areas of the cingulate gyrus and the medial frontal lobe. Most areas were equally affected in both hemispheres, with a symmetrical distribution that has been previously described in *MAPT* mutation patients [19, 40]. Using a much more restrictive statistical analysis five regions were consistently associated with mutation status including the left temporal lobe (left amygdala, left temporal pole), bilateral cingulate cortex (left rostral anterior cingulate gyrus, right posterior cingulate), and the lingual gyrus in the occipital lobe.

Until now, studies regarding early structural changes in asymptomatic *MAPT* carriers have shown

inconsistent results: while several small case series had reported neuroimaging differences in asymptomatic subjects, other studies did not find any structural change [40, 41]. Those studies that found differences point to early degeneration in the temporal lobe, medial frontal lobe, and cingulate cortex. An earlier study, published in 2010 by Miyoshi et al. [21], found the medial temporal lobe and cingulate gyrus affected (hippocampal atrophy and striatal dopaminergic dysfunction). The most recent work shows also emerging grey matter temporal lobe changes in *MAPT* asymptomatic mutation carriers [42]. Our results agree partially with these findings as well as with the largest study in asymptomatic mutation carriers to date [19, 20], which found differences in hippocampal and amygdala volumes as early as 15 years prior to expected symptom onset, in the temporal lobe 10 years before expected onset and in insula 5 years before expected symptom onset. However, after correction for multiple comparisons, only changes in the insular area remained significant. Ours study supports these previous results, confirming differences in hippocampus, amygdala, the insular area, and temporal lobe between carriers and non-carriers, which survived correction for multiple comparisons. Moreover, we found significant differences between basal ganglia volume (caudate, putamen), some areas of the frontal lobe, and the cingulate gyrus. Our results survived multiple comparison correction even though we applied a much more restrictive statistical method in order to determine the strongest association with mutation status. If we consider only the elastic-net model results, the amygdala and temporal lobe remain affected in our sample, whereas there were no differences for hippocampus and insula volumes. Considering that the insula was the last structure affected in the GENFI study, it is possible that the carriers in our cohort had not yet reached that stage of progression. Both studies have important differences regarding sample characteristics, statistical methodology, and imaging analysis. Our sample includes fewer asymptomatic carriers than the GENFI study; however, subjects came from only five families carrying five mutations, as opposed to the GENFI 17 different families of *MAPT* carriers carrying ten different mutations. Considering that FTD is a protean pathology [11] in which disease phenotypes may vary substantially between families and individuals with different mutations [43], our sample's characteristics can add to the body of knowledge currently available. Regarding neuroimaging, our study was performed at only three sites and we used only one type of MRI scan, which increases the consistency of the results. We examined the volume not only of the brain lobes as a whole, but also of specific areas in each lobe. Regarding white matter changes, our results agree with the findings of the GENFI cohort [26], which did not report any difference in white matter hyperintensities either in clinical and preclinical MAPT mutation carriers when compared to controls. Interestingly, our analysis was performed using FLAIR sequence, which is the standard for the study of white matter hyperintensities and is usually available in clinical practice, while the initial GENFI cohort used T2-weighted images. Since white matter hyperintensities do not reflect white matter integrity, we performed DTI analysis in our sample, where we did not find significant differences in our groups after adjusting for age. Previous studies have found white matter involvement in *MAPT* mutation patients [22–25], particularly in the uncinate fasciculus [42, 44]. A recent study published in 2019 showed a disproportional volume loss of the right temporal lobe and more fractional anisotropy decline in the uncinate fasciculus of MAPT carriers converting to clinical FTD [45]. This study includes a follow-up phase and compares converters, non-converters, and non-carriers. Differences between groups were only evident 2 years before symptom onset, while 4 years before symptom onset these differences did not exist. In our study we did not differentiate converters and non-converters and we performed one cross-sectional analysis, without controlling for time to onset. These methodological disparities could explain the different results regarding white matter integrity.

Studies performed in symptomatic subjects have been much more numerous, although once the disease is clinically noticeable, structural changes are generally widespread. Moreover, many of these studies are performed in sporadic forms of the disease, which may differ from genetic cases. However, neuropathological studies performed in sporadic FTD patients who died early in the course of their illness [5] show atrophy in some of the areas affected in our study: the frontal lobe, the medial temporal lobe (hippocampus, amygdala), and anterior cingulate gyrus. Some authors studying specifically neuroimaging changes in *MAPT* mutation patients [8, 40] report predominant gray matter loss in the temporal lobe, particularly the anterior and medial temporal lobe, with varying degrees of frontal and parietal lobe involvement in clinically diagnosed FTD. The orbitofrontal cortex, ventral insula, and anterior cingulate have also been found affected [7]. When subjects with mutations

in the *MAPT* gene show a widespread pattern of frontotemporal gray matter loss, the most severely affected regions are the anteromedial temporal lobes, suggesting that this may be the first area affected by the disease [8]. *MAPT* patients tend to show symmetric patterns of atrophy [46], with no differences between left and right hemisphere when comparing bilateral regions of interest. This is consistent with our sample of preclinical mutation carriers where most areas in both hemispheres were also equally affected, suggesting that the disease begins and progresses symmetrically.

Overall, the atrophy profile observed in *MAPT* patients involves a ventral orbitofrontal-medial temporal-ventral insula network [9]. Dysfunction of this network has been associated with poor performance on memory and naming, executive dysfunction, and language deficits, widely recognized in FTD [47]. Patients commonly develop semantic impairment later in the disease, as well as prominent episodic memory difficulties [9]. Other structures affected in our sample (amygdala and cingulate cortex) belong to the rostral limbic system, which has been suggested to underlie FTD symptoms [47]. This system integrates limbic structures with output-related structures: the amygdala processes the value of internal and external stimuli, represents that value in the form of emotion to the brain and associates this emotion to external stimuli. Moreover, the amygdala, in close connection with the ventromedial prefrontal and anterior cingulate cortices, contributes to other higher order functions such as decision-making, theory of mind, and emotional processing [48, 49], while the anterior section of the cingulate cortex detects conflict within ongoing information processing and integrates information from different structures of the circuit [50].

There is evidence that early changes in connectivity could precede the occurrence of regional atrophy. Some authors studied asymptomatic mutation carriers using functional neuroimaging and reported changes in connectivity, metabolic structure, and blood flow without structural changes [18], suggesting that structural imaging changes may appear after deficits in functional networks have been going on for some time. Alberici et al. [51] reported significant reductions of frontal lobe blood flow (dorsolateral frontal cortex, frontal poles, and mesial frontal cortex) in an asymptomatic *P301L* mutation carrier using SPECT, although these changes were not evident in structural brain imaging. Dopper and colleagues [41] reported frontal, posterior temporal, and parietal hypoperfusion in asymptomatic *MAPT* and *GRN* mutation carriers. Whitwell et al. [18] compared functional connectivity in *MAPT* mutation carriers, healthy controls, and bvFTD patients. Although there was no significant reduction of salience network connectivity in *MAPT* carriers, there was a suggestion of reduced connectivity in the anterior cingulate, one of the areas affected in our cohort's *MAPT* mutation carriers. The aforementioned studies suggest that once changes are noticeable using structural neuroimaging, deficits in functional brain networks may have been going on for some time.

This study was performed in a well-characterized and broadly phenotyped group of asymptomatic *MAPT* mutation carriers and familial matched controls. We would like to remark the strength of our findings: *MAPT* carriers and controls were recruited from the offspring generation of only five families, and were matched by age and family for analyses. Age, sex, and education were included in all analyses as covariates to further reduce potential confounds. The differences we found between carriers and non-carriers survived multiple comparisons and elastic/net analysis. Nevertheless, there were limitations to our study. First, our cohort is small when compared to previous studies. Second, although none of our carriers met diagnostic criteria for FTD, some of them received a CDR score of 0.5 for questionable symptoms and it is arguable if we can describe these patients as pre-symptomatic or if defining an MCI-FTD stage subgroup could be more appropriate. A CDR 0.5 allows a suspicion of early dementia, meaning that the subject shows consistent changes in cognitive function or functional impairments, even if they do not fulfill diagnostic criteria for FTD. It would be also desirable to know the expected time to onset for each subject, as it was reported in previous studies, and it would also help clarify the meaning of the CDR 0.5 subjects in this sample. As the specific underlying mutation may affect the pattern of atrophy [40], a subgroup analysis would have been desirable, but this was not possible due to the size of our sample. Specifically, patients carrying IVS10 + 16, IVS10 + 3, N279K, and S305N mutations show the most severe grey matter loss in the anterior temporal lobe, especially the medial structures. Patients with P301L or V337M mutations also show severe gray matter loss in the anterior temporal lobe, but unlike in our study, with a relative sparing of the medial temporal lobe and greater atrophy observed in more inferior and lateral temporal regions [40]. In addition, there is evidence that P301L and V337M FTD

patients exhibit severe atrophy of the basal ganglia, a finding that was observed in our cohort of *MAPT* mutation carriers as a whole. These differences in patterns of atrophy between *MAPT* mutations may be secondary to their effects in the splicing of exon 10 and in the structural and functional properties of the resulting tau protein [52]. Larger samples exploring how different mutations result in diverse atrophy profiles are needed.

In conclusion, this study provides additional data regarding early structural changes in a homogeneous sample of preclinical *MAPT* mutation carriers, adding to previous reports [20]. In our sample, atrophy was detected in preclinical mutation carriers compared to related non-carriers. Temporal lobe (left amygdala, left temporal pole), cingulate cortex (left rostral anterior cingulate gyrus, right posterior cingulate), and the lingual gyrus seem to be early targets of the disease. Regarding white matter, we did not find differences in white matter hyperintensities or DTI analysis after adjusting for age.

Although this cross-sectional study offers valuable information, we continue to follow these patients in a longitudinal study design so we can assess atrophy rates across time. The degree to which FTD spreads between neighboring regions of the brain versus following a functional network comprised of spatially separated brain regions is still under investigation.

SUPPLEMENTARY MATERIAL

The supplementary material is available in the electronic version of this article: https://dx.doi.org/10.3233/JAD-190820.

REFERENCES

[1] Knopman DS, Roberts RO (2011) Estimating the number of persons with frontotemporal lobar degeneration in the US population. *J Mol Neurosci* **45**, 330-335.

[2] Rohrer JD, Guerreiro R, Vandrovcova J, Uphill J, Reiman D, Beck J, Isaacs AM, Authier A, Ferrari R, Fox NC, Mackenzie IR, Warren JD, de Silva R, Holton J, Revesz T, Hardy J, Mead S, Rossor MN (2009) The heritability and genetics of frontotemporal lobar degeneration. *Neurology* **73**, 1451-1456.

[3] Rohrer JD, Warren JD (2011) Phenotypic signatures of genetic frontotemporal dementia. *Curr Opin Neurol* **24**, 542-549.

[4] Whitwell JL, Weigand SD, Boeve BF, Senjem ML, Gunter JL, DeJesus-Hernandez M, Rutherford NJ, Baker M, Knopman DS, Wszolek ZK, Parisi JE, Dickson DW, Petersen RC, Rademakers R, Jack CR Jr, Josephs KA (2012) Neuroimaging signatures of frontotemporal dementia genetics: C9ORF72, tau, progranulin and sporadics. *Brain* **135**, 794-806.

[5] Kril JJ, Halliday GM (2004) Clinicopathological staging of frontotemporal dementia severity: Correlation with regional atrophy. *Dement Geriatr Cogn Disord* **17**, 311-315.

[6] Mahoney CJ, Beck J, Rohrer JD, Lashley T, Mok K, Shakespeare T, Yeatman T, Warrington EK, Schott JM, Fox NC, Rossor MN, Hardy J, Collinge J, Revesz T, Mead S, Warren JD (2012) Frontotemporal dementia with the C9ORF72 hexanucleotide repeat expansion: Clinical, neuroanatomical and neuropathological features. *Brain* **135**, 736-750.

[7] Rohrer JD, Ridgway GR, Modat M, Ourselin S, Mead S, Fox NC, Rossor MN, Warren JD (2010) Distinct profiles of brain atrophy in frontotemporal lobar degeneration caused by progranulin and tau mutations. *Neuroimage* **53**, 1070-1076.

[8] Whitwell JL, Jack CR Jr, Boeve BF, Senjem ML, Baker M, Rademakers R, Ivnik RJ, Knopman DS, Wszolek ZK, Petersen RC, Josephs KA (2009) Voxel-based morphometry patterns of atrophy in FTLD with mutations in MAPT or PGRN. *Neurology* **72**, 813-820.

[9] Seeley WW, Crawford R, Rascovsky K, Kramer JH, Weiner M, Miller BL, Gorno-Tempini ML (2008) Frontal paralimbic network atrophy in very mild behavioral variant frontotemporal dementia. *Arch Neurol* **65**, 249-255.

[10] Van Swieten J, Spillantini MG (2007) Hereditary frontotemporal dementia caused by Tau gene mutations. *Brain Pathol* **17**, 63-73.

[11] Ghetti B, Oblak AL, Boevet BF, Johnson KA, Dickerson BC, Goedert M (2015) Invited review: Frontotemporal dementia caused by *microtubule-associated protein tau (MAPT)* mutations: A chameleon for neuropathology and neuroimaging. *Neuropathol Appl Neurobiol* **41**, 24-46.

[12] Cheran G, Silverman H, Manoochehri M, Goldman J, Lee S, Wu L, Cines S, Fallon E, Kelly BD, Olszewska DA, Heidebrink J, Shair S, Campbell S, Paulson H, Lynch T, Cosentino S, Huey ED (2017) Psychiatric symptoms in preclinical behavioural-variant frontotemporal dementia in *MAPT* mutation carriers. *J Neurol Neurosurg Psychiatry* **89**, 449-455.

[13] Eskildsen SF, Østergaard LR, Rodell AB, Østergaard L, Nielsen JE, Isaacs AM, Johannsen P (2009) Cortical volumes and atrophy rates in FTD-3 CHMP2B mutation carriers and related non-carriers. *Neuroimage* **45**, 713-721.

[14] Rohrer JD, Ahsan RL, Isaacs AM, Nielsen JE, Ostergaard L, Scahill R, Warren JD, Rossor MN, Fox NC, Johannsen P; FReJA consortium (2009) Presymptomatic generalized brain atrophy in frontotemporal dementia caused by CHMP2B mutation. *Dement Geriatr Cogn Disord* **27**, 182-186.

[15] Lunau L, Mouridsen K, Rodell A, Ostergaard L, Nielsen JE, Isaacs A, Johannsen P; FReJA Consortium (2012) Presymptomatic cerebral blood flow changes in CHMP2B mutation carriers of familial frontotemporal dementia (FTD-3), measured with MRI. *BMJ Open* **2**, e000368.

[16] Walhout R, Schmidt R, Westeneng HJ, Verstraete E, Seelen M, van Rheenen W, de Reus MA, van Es MA, Hendrikse J, Veldink JH, van den Heuvel MP, van den Berg LH (2015) Brain morphologic changes in asymptomatic C9orf72 repeat expansion carriers. *Neurology* **85**, 1780-1788.

[17] Pievani M, Paternicò D, Benussi L, Binetti G, Orlandini A, Cobelli M, Magnaldi S, Ghidoni R, Frisoni GB (2014) Pattern of structural and functional brain abnormalities in asymptomatic granulin mutation carriers. *Alzheimers Dement* **10**, S354-S63 e1.

[18] Whitwell JL, Josephs KA, Avula R, Tosakulwong N, Weigand SD, Senjem ML, Vemuri P, Jones DT, Gunter JL, Baker M, Wszolek ZK, Knopman DS, Rademakers R, Petersen RC, Boeve BF, Jack CR Jr (2011) Altered functional connectivity in asymptomatic MAPT subjects: A comparison to bvFTD. *Neurology* **77**, 866-874.

[19] Rohrer JD, Nicholas JM, Cash DM, van Swieten J, Dopper E, Jiskoot L, van Minkelen R, Rombouts SA, Cardoso MJ, Clegg S, Espak M, Mead S, Thomas DL, De Vita E, Masellis M, Black SE, Freedman M, Keren R, MacIntosh BJ, Rogaeva E, Tang-Wai D, Tartaglia MC, Laforce R Jr, Tagliavini F, Tiraboschi P, Redaelli V, Prioni S, Grisoli M, Borroni B, Padovani A, Galimberti D, Scarpini E, Arighi A, Fumagalli G, Rowe JB, Coyle-Gilchrist I, Graff C, Fallström M, Jelic V, Ståhlbom AK, Andersson C, Thonberg H, Lilius L, Frisoni GB, Pievani M, Bocchetta M, Benussi L, Ghidoni R, Finger E, Sorbi S, Nacmias B, Lombardi G, Polito C, Warren JD, Ourselin S, Fox NC, Rossor MN, Binetti G (2015) Presymptomatic cognitive and neuroanatomical changes in genetic frontotemporal dementia in the Genetic Frontotemporal dementia Initiative (GENFI) study: A cross-sectional analysis. *Lancet Neurol* **14**, 253-262.

[20] Cash DM, Bocchetta M, Thomas DL, Dick KM, van Swieten JC, Borroni B, Galimberti D, Masellis M, Tartaglia MC, Rowe JB, Graff C, Tagliavini F, Frisoni GB, Laforce R Jr, Finger E, de Mendonça A, Sorbi S, Rossor MN, Ourselin S, Rohrer JD (2018) Genetic FTD Initiative, GENFI. Patterns of gray matter atrophy in genetic frontotemporal dementia: Results from the GENFI study. *Neurobiol Aging* **62**, 191-196.

[21] Miyoshi M, Shinotoh H, Wszolek ZK, Strongosky AJ, Shimada H, Arakawa R, Higuchi M, Ikoma Y, Yasuno F, Fukushi K, Irie T, Ito H, Suhara T (2010) *In vivo* detection of neuropathologic changes in presymptomatic MAPT mutation carriers: A PET and MRI study. *Parkinsonism Relat Disord* **16**, 404-408.

[22] Mahoney CJ, Ridgway GR, Malone IB, Downey LE, Beck J, Kinnunen KM, Schmitz N, Golden HL, Rohrer JD, Schott JM, Rossor MN, Ourselin S, Mead S, Fox NC, Warren JD (2014) Profiles of white matter tract pathology in frontotemporal dementia. *Hum Brain Mapp* **35**, 4163-4179.

[23] Tacik P, Sanchez-Contreras M, DeTure M, Murray ME, Rademakers R, Ross OA, Wszolek ZK, Parisi JE, Knopman DS, Petersen RC, Dickson DW (2017) Clinicopathologic heterogeneity in frontotemporal dementia and parkinsonism linked to chromosome 17 (FTDP-17) due to microtubule-associated protein tau (MAPT) p.P301L mutation, including a patient with globular glial tauopathy. *Neuropathol Appl Neurobiol* **43**, 200-214.

[24] Caroppo P, Le Ber I, Camuzat A, Clot F, Naccache L, Lamari F, De Septenville A, Bertrand A, Belliard S, Hannequin D, Colliot O, Brice A (2014) Extensive white matter involvement in patients with frontotemporal lobar degeneration. *JAMA Neurol* **71**, 1562.

[25] Paternicò D, Premi E, Gazzina S, Cosseddu M, Alberici A, Archetti S, Cotelli MS, Micheli A, Turla M, Gasparotti R, Padovani A, Borroni B (2016) White matter hyperintensities characterize monogenic frontotemporal dementia with granulin mutations. *Neurobiol Aging* **38**, 176-180.

[26] Sudre CH, Bocchetta M, Cash D, Thomas DL, Woollacott I, Dick KM, van Swieten J, Borroni B, Galimberti D, Masellis M, Tartaglia MC, Rowe JB, Graff C, Tagliavini F, Frisoni G, Laforce R Jr, Finger E, de Mendonça A, Sorbi S, Ourselin S, Cardoso MJ, Rohrer JD, Genetic FTD Initiative, GENFI (2017) White matter hyperintensities are seen only in GRN mutation carriers in the GENFI cohort. *Neuroimage Clin* **15**, 171-180.

[27] Petersen ET, Mouridsen K, Golay X; all named co-authors of the QUASAR test-retest study (2010) The QUASAR reproducibility study, Part II: Results from a multi-center Arterial Spin Labeling test-retest study. *Neuroimage* **49**, 104-113.

[28] Walhovd KB, Westlye LT, Amlien I, Espeseth T, Reinvang I, Raz N, Agartz I, Salat DH, Greve DN, Fischl B, Dale AM, Fjell AM (2011) Consistent neuroanatomical age-related volume differences across multiple samples. *Neurobiol Aging* **32**, 916-932.

[29] Whitwell JL, Jack CRJ (2005) Comparisons between Alzheimer disease, frontotemporal lobar degeneration, and normal aging with brain mapping. *Top Magn Reson Imaging* **16**, 409-425.

[30] Smith SM, Jenkinson M, Woolrich MW, Beckmann CF, Behrens TEJ, Jihansen-Berg H, Bannister PR, De Luca M, Drobnjak I, Flitney Dem Niazy R, Saunders J, Vickers J, Zhang Y, De Stefano N, Brady JM, Matthews PM (2004) Advances in functional and structural MR image analysis and implementation as FSL. *Neuroimage* **23**, 208-219.

[31] Smith M, Jenkinson M, Johansen-Berg H, Rueckert D, Nichols TE, Mackay CE, Watkins KE, Ciccarelli O, Cader MZ, Matthews PM, Behrens TEJ (2006) Tract-based spatial statistics: Voxelwise analysis of multi-subject diffusion data. *Neuroimage* **31**,1487 1505.

[32] Andersson JLR, Jenkinson M, Smith S (2007) Nonlinear optimisation. FMRIB technical report TR07JA1. http://www.fmrib.ox.ac.uk/analysis/techrep.

[33] Andersson JLR, Jenkinson M, Smith S (2007) Nonlinear registration, aka Spatial normalisation FMRIB technical report TR07JA2. http://www.fmrib.ox.ac.uk/analysis/techrep.

[34] Mori S, Wakana S, van Zijl PCM, Nagae-Poetscher LM (2005) *Atlas of Human White Matter*. Elsevier, Amsterdam.

[35] Friedman J, Hastie T, Tibshirani R (2010) Regularization paths for generalized linear models via coordinate descent. *J Stat Softw 2010* **33**, 1-22. Available at: http://www.jstatsoft.org/v33/i01/.

[36] Robin X, Turck N, Hainard A, Tiberti N, Lisacek F, Sanchez JC, Müller M (2011) pROC: An open-source package for R

and *S*+ to analyze and compare ROC curves. *BMC Bioinformatics* **12**, 77.

[37] Benjamini Y, Hochberg Y (1995) Controlling the false discovery rate: A practical and powerful approach to multiple testing. *J R Stat Soc Series* **B 57**, 289–300.

[38] Hui Z, Hastie T (2005) Regularization and variable selection via the elastic net. *J R Statist Soc B* **67**(Pt 2), 301-320.

[39] Knopman DS, Kramer JH, Boeve BF, Caselli RJ, Graff-Radford NR, Mendez MF, Miller BL, Mercaldo N (2008) Development of methodology for conducting clinical trials in frontotemporal lobar degeneration. *Brain* **131**, 2957-2968.

[40] Whitwell JL, Jack CR Jr, Boeve BF, Senjem ML, Baker M, Ivnik RJ, Knopman DS, Wszolek ZK, Petersen RC, Rademakers R, Josephs KA (2009) Atrophy patterns in IVS10+16, IVS10+3, N279K, S305N, P301L, and V337M MAPT mutations. *Neurology* **73**, 1058-1065.

[41] Dopper EG, Chalos V, Ghariq E, den Heijer T, Hafkemeijer A, Jiskoot LC, de Koning I, Seelaar H, van Minkelen R, van Osch MJ, Rombouts SA, van Swieten JC (2016) Cerebral blood flow in presymptomatic MAPT and GRN mutation carriers: A longitudinal arterial spin labeling study. *Neuroimage Clin* **12**, 460-465.

[42] Panman JL, Jiskoot LC, Bouts MJRJ, Meeter LHH, van der Ende EL, Poos JM, Feis RA, Kievit AJA, van Mikelen R, Dopper EGP, Rombouts SARB, van Swieten JC, Papma JM (2019) Gray and white matter changes in presymptomatic genetic frontotemporal dementia: A longitudinal MRI study. *Neurobiol A*ging **76**, 115-124.

[43] Forman MS (2004) Genotype-phenotype correlations in FTDP-17: Does form follow function? *Exp Neurol* **187**, 229-234.

[44] Jiskoot LC, Bocchetta M, Nicholas JM, Cash DM, Thomas D, Modat M, Ourselin S, Rombouts SARB, Dopper EGP, Meeter LH, Panman JL, van Minkelen R, van der Ende EL, Donker Kaat L, Pijnenburg YAL, Borroni B, Galimberti D, Masellis M, Tartaglia MC, Rowe J, Graff C, Tagliavini F, Frisoni GB, Laforce R Jr, Finger E, de Mendonça A, Sorbi S, on behalf of the Genetic Frontotemporal dementia Initiative (GENFI), Papma JM, van Swieten JC, Rohrer JD (2018) Presymptomatic white matter integrity loss in familial frontotemporal dementia in the GENFI cohort: A cross-sectional diffusion tensor imaging study. *Ann Clin Transl Neurol* **5**, 1025-1036.

[45] Jiskoot LC, Panman JL, Meeter LH, Dopper EGP, Donker Kaat L, Franzen S, van der Ende EL, van Minkelen R, Rombouts SARB, Papma JM, van Swieten JC (2019) Longitudinal multimodal MRI as prognostic and diagnostic biomarker in presymptomatic familial frontotemporal dementia. *Brain* **142**, 193-208.

[46] Van Deerlin VM, Wood EM, Moore P, Yuan W, Forman MS, Clark CM, Neumann M, Kwong LK, Trojanowski JQ, Lee VM, Grossman M (2007) Clinical, genetic, and pathologic characteristics of patients with frontotemporal dementia and progranulin mutations. *Arch Neurol* **64**, 1148-1153.

[47] Boccardi M, Sabattoli F, Laakso MP, Testa C, Rossi R, Beltramello A, Soininen H, Frisoni GB (2005) Frontotemporal dementia as a neural system disease. *Neurobiol Aging* **26**, 37-44.

[48] Cardinal RN, Parkinson JA, Hall J, Everitt, BJ (2002) Emotion and motivation: The role of the amygdala, ventral striatum, and prefrontal cortex. *Neurosci Biobehav Rev* **26**, 321-352.

[49] Stone VE, Baron-Cohen S, Calder A, Keane J, Young A (2003) Acquired theory of mind impairments in individuals with bilateral amygdala lesions. *Neuropsychologia* **41**, 209-220.

[50] Devinsky O, Morrell MJ, Vogt BA (1995) Contributions of anterior cingulate cortex to behavior. *Brain* **118**, 279-306.

[51] Alberici A, Gobbo C, Panzacchi A, Nicosia F, Ghidoni R, Benussi L, Hock C, Papassotiropoulos A, Liberini P, Growdon JH, Frisoni GB, Villa A, Zanetti O, Cappa S, Fazio F, Binetti G (2004) Frontotemporal dementia: Impact of P301L tau mutation on a healthy carrier. *J Neurol, Neurosurg Psychiatry* **75**, 1607-1610.

[52] Goedert M, Jakes R (2005) Mutations causing neurodegenerative tauopathies. *Biochim Biophys Acta* **1739**, 240-250.